Directional Measurements and Propagation Models at 28 GHz for Reliable Factory Coverage

Dmitry Chizhik, *Fellow, IEEE*, Jinfeng Du, *Member, IEEE*, Reinaldo A. Valenzuela, *Fellow, IEEE*, Dragan Samardzija, Stepan Kucera, *Senior Member, IEEE*, Dmitry Kozlov, Rolf Fuchs, Juergen Otterbach, Johannes Koppenborg, Paolo Baracca, *Member, IEEE*, Mark Doll, Ignacio Rodriguez, *Member, IEEE*, Rodolfo Feick, *Life Senior Member, IEEE*, and Mauricio Rodriguez, *Senior Member, IEEE*

***Abstract*— Directional measurements of over 2600 links in four distinct factories at 28 GHz are used to formulate the path gain and azimuth gain models to allow reliable 90% coverage estimates. A simple theoretical model of path gain, dependent on ceiling and clutter heights, is found to represent path gain across the four factories with 4.4 dB root-mean-square error (RMSE), contrasted with 6.9 dB slope-intercept fit and 8.5–14.9 dB RMSE for 3GPP factory models. The model also did well against 3.5 GHz path loss data collected over 18 MHz bandwidth in one of the factories, with an RMSE of 3.3 dB. In nonline-of-sight (NLOS) conditions, scattering reduces available antenna azimuth gain from nominal value by up to 7.3 dB in 90% of links. Line-of-sight (LOS) blockage by a 1.7 m × 1 m obstacle in factory aisle leads to 7 dB signal reduction, attributed to availability of other paths. It is found that an access point (AP) using 25 dBm transmit power per polarization, with 23 dBi nominal gain and omnidirectional terminals, supporting 2 × 2 MIMO in a 400 MHz bandwidth, can provide 130 Mb/s for 90% of factory locations within 50 m.**

***Index Terms*— Factory, industrial Internet of Things (IIoT), measurement, path loss, propagation.**

I. Introduction

PROVIDING coverage for high-rate links in mmWave bands is of particular interest in factory environments for the industrial Internet of Things (IIoT) applications. Coverage range critically depends on path gain and available antenna directional gain. Accurate prediction of these quantities is important for planning and deploying wireless communication networks. Path gain as a function of range is typically predicted using slope-intercept formulas, with these two parameters determined from linear fit to measurements conducted in similar environments [3]. Antenna performance is determined by scattering, often characterized through angle spread.

The 3GPP 38.901 standardization document [3] provides a path gain model in the range 0.5–100 GHz with four types of factory environments, with combinations of sparse and dense clutter and with access point (AP) antennas above and below clutter ("high" and "low" antennas). Extensive measurements in several industrial settings were conducted by NIST [4], [5], at 2.2 and 5.4 GHz, providing path gain versus range models for individual data runs, with distance exponents ranging from 3.2 to 5.0.

In the present work, we report directional measurements and propagation models from extensive measurement campaigns in four-factory buildings, with over 2600 links, 18 million individual power measurements. Measured factory areas did not have wall separations. Ceiling heights in the four factories ranged from 3.3 to 8 m, with average clutter height (height of metal machinery) ranging from 1.5 to 3.5 m. We also provide estimates of coverage in factories at 28 GHz and provide guidance on required antenna gains.

We characterize measured path gain dependence on range using both a conventional slope-intercept model as well as a theoretical model dependent on ceiling and clutter heights and a (fixed) absorption loss parameter. Line-of-sight (LOS) and nonline-of-sight (NLOS) links are examined separately. We also summarize statistically the distribution of measured effective antenna gains, degraded by scattering.

The effect of LOS blockage by an obstacle appearing in a factory aisle was assessed experimentally to quantify the impact on the link budget.

Statistical models formulated based on analysis of the experimental results are then used to assess coverage and achievable rate in factories and provide guidance on the value of using directional antennas in factory environments.

The key contributions of this article include the following.

1) Path gain and azimuth gain models derived from over 2600 link measurements in four distinct factory

Manuscript received 20 December 2021; accepted 22 April 2022. Date of publication 30 May 2022; date of current version 9 November 2022. The work of Rodolfo Feick was supported by the Chilean Research Agency ANID under Grant PIA/APOYO AFB180002 and Grant ANID/REDES 180144. The work of Mauricio Rodriguez was supported in part by the Chilean Research Agency ANID under Grant ANID FONDECYT 1211368, Grant ANID FONDEQUIP EQM190023, and Grant ANID PIA/APOYO AFB180002; and in part by the project under Grant VRIEA-PUCV 039.437/2020. *(Corresponding author: Dmitry Chizhik.)*

Dmitry Chizhik, Jinfeng Du, Reinaldo A. Valenzuela, and Dragan Samardzija are with Nokia Bell Labs, Murray Hill, NJ 07974 USA (e-mail: dmitry.chizhik@nokia-bell-labs.com).

Stepan Kucera is with Nokia Bell Labs Munich, 81541 Munich, Germany.

Dmitry Kozlov is with Nokia Technology Center, 89081 Ulm, Germany.

Rolf Fuchs, Juergen Otterbach, Johannes Koppenborg, Paolo Baracca, and Mark Doll are with Nokia Bell Labs Stuttgart, D-70469 Stuttgart, Germany.

Ignacio Rodriguez is with the Department of Electronic Systems, Aalborg University, 9220 Aalborg, Denmark.

Rodolfo Feick is with the Department of Electronics Engineering, Universidad Tecnica Federico Santa Maria, Valparaíso 2390123, Chile.

Mauricio Rodriguez is with the Escuela de Ingeniería Eléctrica, Pontificia Universidad Catolica de Valparaíso, Valparaíso 2362804, Chile.

Color versions of one or more figures in this article are available at https://doi.org/10.1109/TAP.2022.3177546.

Digital Object Identifier 10.1109/TAP.2022.3177546

buildings to allow reliable estimates of 90% coverage. The corresponding 3GPP models are found to predict 6–10 dB less loss than the measured one here.

2) Simple path gain formula derived from physics requires only ceiling and clutter heights as inputs. The new formula reproduces diverse path gain results from the four factories with 4.4 dB rms error, compared to 6.9 dB rms from an overall data fit and 8.5–14.9 dB rms from 3GPP factory models. The model remained accurate against 3.5 GHz wideband data collected in one of the factories with a 3.3 dB rms error.
3) Blockage of LOS by a 1.7 m × 1 m obstacle in a factory aisle results in a modest 7 dB reduction in signal strength, attributed to the availability of other paths.
4) Estimation of coverage using antennas with practical gains in realistic conditions, providing a way to assess the value of using directional antennas in a scattering environment.

II. Measurement Description

We used a narrowband sounder [6], transmitting a 28 GHz continuous wave (CW) tone at 22 dBm into an omnidirectional (omni) antenna. The receiver antenna is a 10° half-power beamwidth (elevation and azimuth), 24 dBi horn.

Measurements were done in four-factory buildings, each typically 100 m × 50 m, with ceiling heights ranging from 3.3 to 8 m. Machinery (large, irregularly shaped metal enclosures) ranged in height from 1.5 to 3.5 m from factory to factory. Rows of machinery were separated by aisles with widths varying from 1.5 to 3 m.

The transmitter with the omnidirectional antenna was placed 1 m above the factory floor, emulating a mobile terminal. The 10° horn receiver, spinning up to 300 r/min, was placed 2.3–2.6 m above the floor, close to ceiling supports in positions that would correspond to an AP. The receiver was moved along a factory aisle, stopping every 1 m to collect measurements at ranges from 1 up to 140 m from the user terminal. At each link, recorded data consisted of received power versus azimuth, allowing estimation of both path gain and effective azimuth gain. Over 2600 link measurements were made. Typical measurement runs are shown in Fig. 1.

III. Measured Path Gain in LOS Factory Aisles

Path gain measurements were conducted in LOS conditions in a factory aisle, with the omnidirectional Tx antenna placed at one end of an aisle, while the spinning Rx horn was moved in 1 m increments up to a range of 140 m.

The measured LOS path gain is plotted versus distance in Fig. 2 for over 500 links in five aisles in four factories, along with least mean square (LMS) linear (slope and intercept) fit to data, as well as Friis free-space path gain. Different symbols correspond to different aisles. The Friis free-space formula predicts the measured path gain with an root-mean-square error (RMSE) of 4.2 dB, close to 4.0 dB rms variation around linear fit. The two lines are within 1 dB of each other. The observed variation is attributed to interference between the direct path and arrivals reflected/scattered from the floor, ceiling, and machinery.

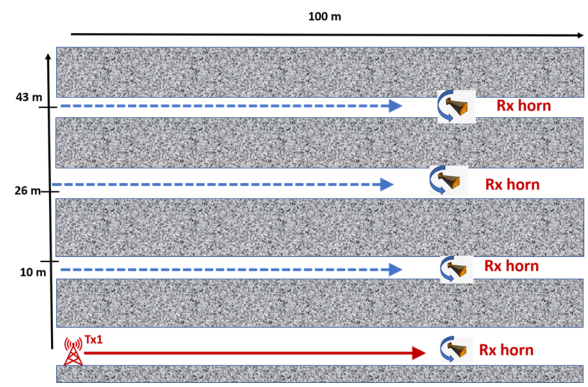

Fig. 1. Measurement geometry of typical links in a factory where the rotating Rx horn moves along the LOS (red solid line) and NLOS (blue dashed lines) trajectories for a fixed omniTx location.

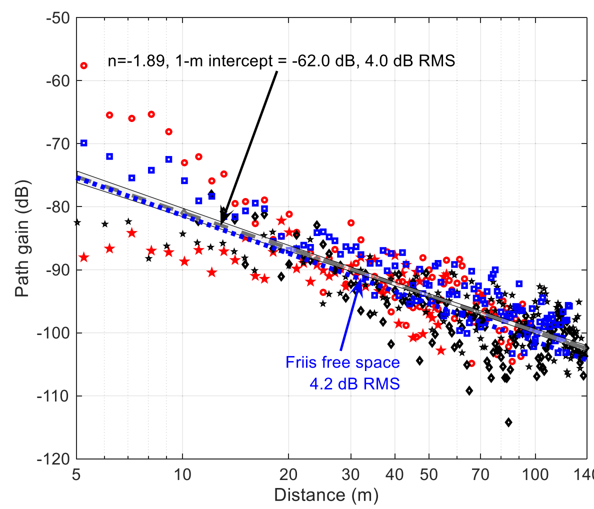

Fig. 2. LOS path gain of over 500 links in five factory aisles at 28 GHz. Data from different aisles are distinguished by different symbols.

IV. Measured Path Gain in NLOS Factory Links

Path gain and azimuthal patterns were measured in over 2000 NLOS links in four-factory buildings, with varying clutter and ceiling heights. In a typical arrangement, the omnidirectional transmitter was placed at a location, while the spinning receiver was moved along aisles separated from the Tx by factory clutter, for example, along the blue dashed lines in Fig. 1. About ten different Tx locations and over 40 factory aisles were measured, at ranges varying from 10 to 130 m. The overall dataset conditions are summarized in Table I. “Heavy clutter” height is the average height of machinery in each factory.

The resulting path gain for each factory is plotted against Tx–Rx separation in Figs. 3–6. “Theory” lines also plotted are described in Section V. The steep drop sections near 60 m distance in Fig. 4 correspond to NLOS data in the vicinity of an intersection of two factory aisles: received power drops steeply with distance as the terminal moves further away from the corner, at a rate consistent with corner diffraction, similar to an intersection of two indoor corridors [6], [7].

TABLE I
NLOS DATASET AND ENVIRONMENTAL PARAMETERS IN THE FOUR FACTORIES

	Number of NLOS links	Ceiling height (m)	Heavy clutter height (m)
Factory 1	91	3.3	2.4
Factory 2	124	5.2	3.1
Factory 3	633	5.0	1.5
Factory 4	1255	8.0	3.5

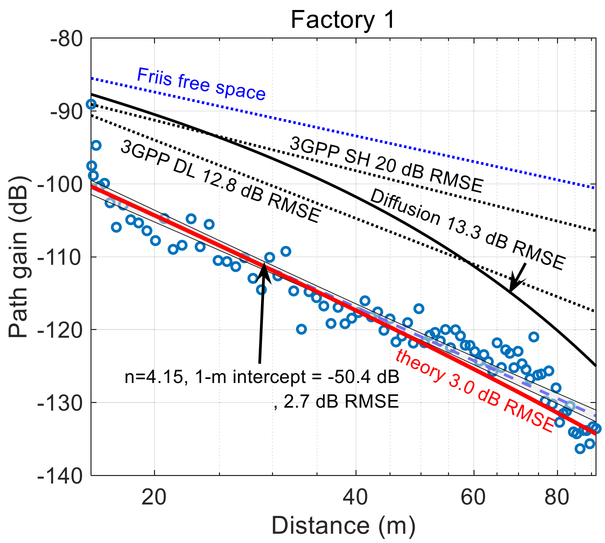

Fig. 3. Measured path gain of all NLOS links at 28 GHz in factory 1. "Theory" is (2).

Figs. 3–6 also show two 3GPP factory ("inF") models, 3GPP-SH ("Sparse High") and 3GPP DL ("Dense Low"), referring to clutter density and AP or terminal height relative to clutter. These are, correspondingly, least lossy and most lossy of the four 3GPP factory models.

A generic slope-intercept path gain model has the form

$$P = A - 10n \log_{10} d + N\left(0, \sigma^2\right). \quad (1)$$

The 1 m intercept A and distance exponent n are determined through an LMS fit to data, with goodness of fit characterized by standard deviation σ. The results of such a fit to the NLOS path gain measurements in these four factories are summarized in Table II and plotted in Figs. 3–6. The gray regions surrounding the slope-intercept fit lines in Figs. 3–6 indicate a 90% confidence region of the fit [11]. Since the receive and transmit antennas were placed at different heights, it is important to make sure that the data used in the analysis correspond to locations within the elevation beamwidth of the antennas. To do that, only data collected at distances beyond 10 m were included in this work to make sure that the locations fall within the 10° elevation beamwidth of the receive antenna.

Path gain distance exponents in Table II are within the range 3.3–4.9 of path gain exponents found at 2.2 and 5.4 GHz in [5]. It may be observed by comparing the fit lines in Figs. 3–6 that the path gain is highly variable from factory to factory, with fit lines spanning 14 dB range at 50 m, as shown in

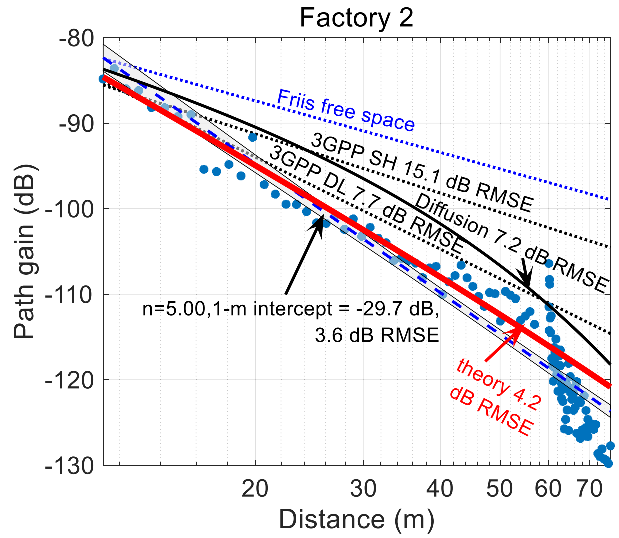

Fig. 4. Measured path gain of all NLOS links at 28 GHz in factory 2. "Theory" is (2).

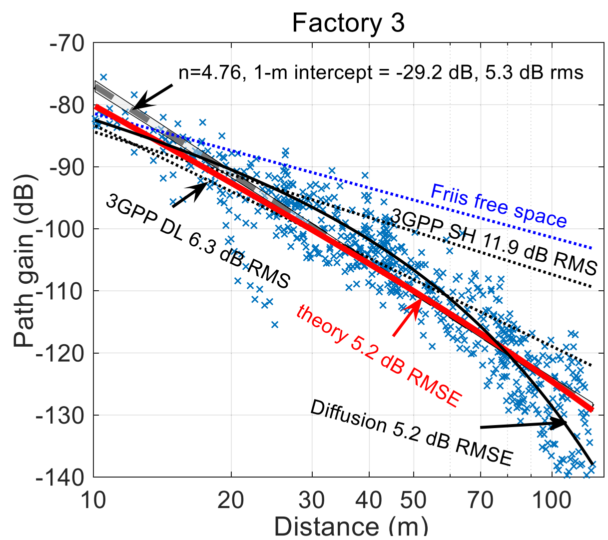

Fig. 5. Measured path gain of all NLOS links at 28 GHz in factory 3.

TABLE II
LMS LINEAR FIT TO 28 GHZ PATH GAIN DATA IN FOUR FACTORIES

	1-m intercept A (dB)	Distance exponent n	RMS fit σ (dB)
Factory 1	-50.4	4.15	2.7
Factory 2	-29.7	5.00	3.6
Factory 3	-29.2	4.76	5.3
Factory 4	-38.2	4.06	5.0
All 4 factories	-43.9	4.07	6.9

Fig. 7. The data from all four factories are combined into a joint dataset and then fitted with a slope intercept to produce a simple joint model, whose parameters are on the last line in Table II. Creation of a joint dataset from an equal number of samples from each environment (here factory) would be a simple union of all measurements.

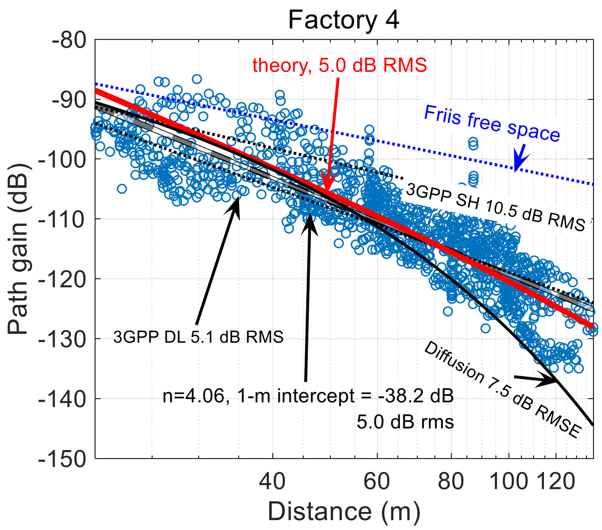

Fig. 6. Measured path gain of all NLOS links at 28 GHz in Factory 4.

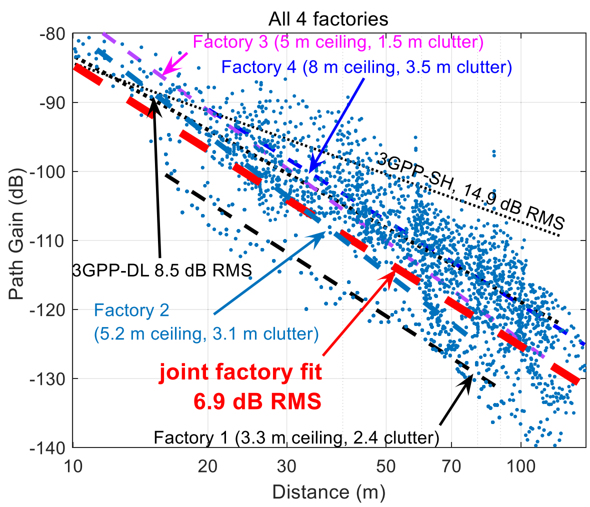

Fig. 7. Joint NLOS path gain data from all four factories, with individual factory line fits superimposed.

We note that expanding a dataset by just accumulating multiple copies of it preserves its cumulative distribution. Since the dataset sizes varied from 91 links to over 1200 links in the four factories measured, a joint dataset was created by repeating each dataset, as necessary, to get approximately the same number of samples from each of the four factories. The resulting (repeated) datasets were then joined into a joint dataset, now with equal representation of each environment.

The fit to data in Factories 1 and 2 (see Figs. 3 and 4) is 7–10 dB below even the "high loss" 3GPP inF-DL (dense clutter and low AP/terminal) model [3], with an rms of 7.7–12.8 dB. The inF-DL model is a better representation of the data in Factories 3 and 4 (see Figs. 5 and 6), with 5.1–6.3 dB rms error. The joint set fit line in Fig. 7 has 6.9 dB rms, while 3GPP-DL and 3GPP-SH have 8.5 and 14.9 dB, respectively. These two models are the ones with the greatest and least loss of the four 3GPP factory models. The other two 3GPP models would thus have accuracies between these limits.

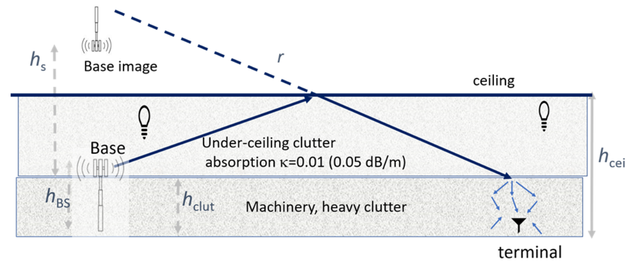

Fig. 8. Factory geometry for theoretical NLOS model.

3GPP recommends choosing the appropriate model dependent on clutter "density." Clutter density is difficult to determine by observation. For instance, it was found here that Factory 4, which appeared (subjectively) to have the densest clutter, also produced the highest path gain (strongest signal) among all the factories, at odds with the corresponding 3GPP model.

V. Theoretical NLOS Path Gain Model for Factories

Wide variation of path gains described in Section IV motivates the development of a theoretical model that can represent such variations based on practically available environment description. In particular, striking observation was that Factory 4 containing the tallest and densest heavy clutter was found to have the lowest losses (strongest coverage) of the four factories. This is in sharp contrast to 3GPP recommendation [3] that placing a base station antenna below average clutter height, in dense clutter (inF-DL in [3]), would produce the highest losses.

It is notable that observed signal levels were found to generally increase with ceiling height in the four factories. This suggested the possibility that the signal from the base is reflecting from the ceiling to reach the general area. The approach to model path gain for this case is here taken as an extension of a model for propagation between an antenna placed in an open space and an antenna placed in a cluttered half-space, developed for the case of a lamppost AP communicating with a terminal placed on an exterior wall of a house, behind foliage [8], itself an extension of [9].

The overall problem is shown in Fig. 8. The factory is viewed as being vertically separated into two regions: lower region, occupied by "heavy" clutter (machinery) of height h_{clut}, and upper region above "heavy clutter" and below ceiling of height h_{ceil}.

The upper region is occupied by a sparse distribution of scatterers (lighting, wiring, air ducts, and structural support), characterized empirically by intrinsic absorption κ.

The terminal placed at a height below h_{clut} is therefore in the lower, "heavy clutter" region.

The propagation from the AP to the terminal is modeled as traversing the "light clutter" upper region, reflecting from the ceiling and penetrating the "heavy clutter" region, where it undergoes strong diffuse scatter from machinery until it reaches the terminal. The corresponding path gain formula, as a function of range r and wavelength λ, is an adaptation of the model for penetrating a cluttered half-space from free half-space [8], modified here to include ground reflection with power reflection coefficient $|\Gamma_g|^2 = 1$

$$P_G = \left(1 + |\Gamma_g|^2\right)\frac{h_s^2 \lambda^2}{8\pi^2 r^4} e^{-\kappa r}. \quad (2)$$

The effective source is the image of the AP antenna due to reflection in the ceiling, at effective "stand-off" height h_s from the heavy clutter region

$$h_s = 2h_{ceil} - h_{clut} - h_{BS}. \quad (3)$$

The path directly illuminating near-terminal clutter can be included by adding to (2) a similar expression, but with the direct standoff distance $h_{s,direct} = h_{BS} - h_{clut}$. This contribution is weaker and is neglected here for simplicity.

Note that part of the propagation path through the upper, "light" clutter, region clears the heavy machinery layer below, as the maximum radius of the first Fresnel zone at 28 GHz is 0.5 m at 100 m range, smaller than the ceiling-clutter separation in all four factories, as observed in Table I. The ceiling-reflected signal path penetrating a cluttered half-space (metal machinery) is a nontrivial extension of the diffusion formula [14] and the direct illumination into vegetation model [8] which treated propagation into suburban vegetation layer, a distinctly different environment.

Loss due to scatter and absorption in the upper region is represented by the factor $e^{-\kappa r}$, with $\kappa = 0.01$, corresponding to 0.05 dB/m, found to provide the best fit to the entire dataset across all four factories. This is the only parameter adjusted to fit the data, as opposed to two parameters needed in the slope-intercept fit. Taking ceiling and clutter height parameters for each of the factories, as tabulated in Table I, to define stand-off height h_s in (3), as well as base height of 2.3–2.6 m, as used in measurements, allows evaluation of (2) for comparison against the four-factory datasets, as shown by the black solid line in Figs. 3–6. The rms model error of (2) is found to vary from 3.0 to 5.2 dB across the four factories.

The accuracies of the slope-intercept fit, theoretical model (2), the diffusion model [14], and 3GPP factory (inF) models [3] are summarized in Table III. The theoretical model (2) has the RMSE of 4.4 dB, compared to 6.9 dB obtained with overall fit, as well as 8.5 dB from the best of the 3GPP factory models ("Dense-Low," inF-DL). The accuracy of (2) may be attributed to its dependence on ceiling and clutter heights. The diffusion model RMSE remained above 8 dB against the overall dataset even after adjusting the absorption parameter κd to an optimal value against the four-factory datasets.

Remark: It might be expected theoretically that the diffusion model [14] might apply in such environments with a statistically uniform distribution of scatterers [12], where absorption losses increase with clutter size and density. Although the diffusion model does well (5.2 dB RMSE) against the Factory 3 data, it is seen here not to generalize well to the other factories studied here (8.8 dB RMSE overall).

Additional path gain measurements were collected at 3.5 GHz in Factory 2 using the same transmitter and receiver locations as the 28 GHz data in Fig. 4. The 3.5 GHz transmitter used a 10 dBm orthogonal frequency division multiplexing

TABLE III
MODEL ACCURACY (RMSE IN dB) AGAINST DATA

data Set	Fit	**Theory (2)**	Diffusion [14]	3GPP-SH	3GPP-DL
Factory 1	2.7	3.0	13.3	20.0	12.8
Factory 2	3.6	4.2	7.2	15.1	7.7
Factory 3	5.3	5.2	5.2	11.9	6.3
Factory 4	5.0	5.0	7.5	10.5	5.1
All	6.9	**4.4**	8.8	14.9	8.5

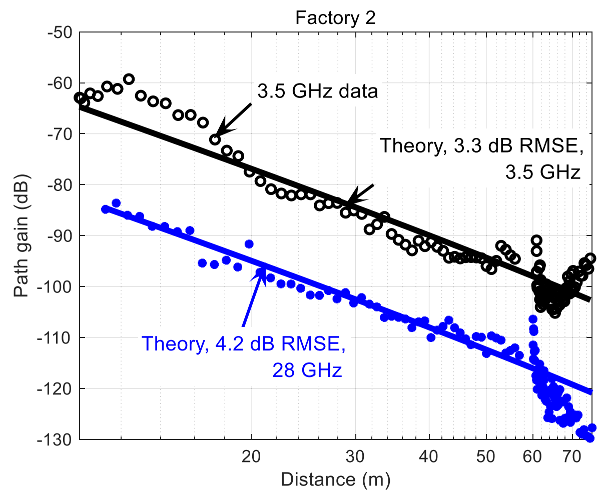

Fig. 9. Measured path gain of all NLOS links at 28 and 3.5 GHz in factory 2. Theory is (2).

(OFDM) signal spread over 18 MHz effective bandwidth, from a 14 dBi (40° half-power beamwidth) vertically polarized antenna placed at 2.6 m above the floor. The received signal was captured using an array of four vertical "whip" 5 dBi antennas, placed pairwise at heights of 0.25 and 1.75 m above the floor, with each pair separated horizontally by 0.25 m. Measured complex channel responses were coherently averaged over time, leading to 29.5 dB processing gain. Path gain was calculated after averaging over the four receivers and 18 MHz bandwidth. Path gains measured at 3.5 and 28 GHz (the same as in Fig. 4) are compared against theory (2) in Fig. 9. The corresponding accuracies are 3.3 dB RMSE at 3.5 GHz and 4.2 dB RMSE at 28 GHz. At 3.5 GHz, the diffusion formula [14] yields 5.1 dB RMSE, 3GPP-SH 14.9 dB, and 3GPP-DL 6.1 dB RMSE. Theory (2) thus maintains its accuracy against available factory data at frequencies that differ by a factor of 8.

VI. EFFECTIVE AZIMUTH GAIN IN NLOS FACTORY LINKS

Scattering generally degrades the effective gain of a directional antenna. Examples of measured azimuthal patterns in LOS and NLOS conditions are shown in Figs. 10 and 11, respectively.

In LOS, the strongest arrival is, unsurprisingly, from the direction of the direct path from the Tx, 180° in Fig. 10, with occasional scattered arrivals from the sides and end of the aisle 5–10 dB weaker than the direct path.

Measured azimuthal power spectra $p(\phi)$ were used to calculate the effective azimuthal gain, which is defined as

$$G_{\mathrm{azim}} = \frac{\max_{\phi} p(\phi)}{\left(1/2\pi\right) \int_0^{2\pi} d\phi p(\phi)}. \tag{4}$$

The cumulative distribution of azimuthal gains in LOS conditions is shown in Fig. 12. It may be observed that 90% of measured azimuth gains are within 3 dB from the 14.5 dB nominal azimuthal gain of the 10° horn, as quantified through (4) from measurements in the anechoic chamber.

The cumulative distributions of azimuthal gains in NLOS for four factories are shown in Fig. 13. Compared to the 14.5 dB nominal, azimuth gain was degraded by up to 7.3 dB for 90% of links across all four factories explored. The empirical distribution of observed directional gain in all four factories in Fig. 13 is within 0.6 dB of a normal distribution with a mean of 9.65 dB and a std. deviation of 1.9 dB. High directional antennas are less effective in fully scattering channels where power versus angle is constant on average, although the angular spectrum instantiation is subject to direction-dependent fading. As a result, modest diversity gains are achievable by selecting the direction with the highest power instantiation, as shown in Fig. 13 where the simulated arrivals from different directions follow the i.i.d. complex Gaussian distribution, as appropriate in full scattering. The amplitude of the complex sum is then Rayleigh distributed. The complex channel spectrum is convolved with the complex antenna pattern [6] measured in an anechoic chamber to generate instantiations of the pattern, whose effective gain is computed using (4) and plotted as the "simulated full scatter" distribution in Fig. 13.

Additional data were collected in Factory 4 at the same set of locations, but with a spinning horn at 1.05 and 2.6 m heights above the floor, to quantify the effect of height on effective azimuth gain. The results in Fig. 14 show the median azimuth gain of about 0.7 dB higher at 2.6 m height than at 1.05 m height. Both heights are below the 3.5 m heavy clutter height, perhaps explaining the small change.

VII. LOS Aisle Blockage in a Factory

Even in nominally LOS conditions, when both Tx and Rx are in the same aisle, the direct signal path may be blocked by an obstacle, such as a person or a forklift. Here, we assess experimentally the impact of LOS blockage in a factory aisle. To do so, a large metal box 1.7 m high × 1 m wide × 0.5 m deep was placed between the Tx and the Rx in a factory aisle, at 2, 5, and 10 m from the Tx. As elsewhere in this work, the Tx was an omnidirectional antenna placed 1 m above the floor, while the spinning horn Rx was mounted under the ceiling at 2.3 m above the floor and moved away from the Tx in 1 m increments, as shown in Fig. 15.

Measured path gain when the blocking plate is 2 m away from the Tx is compared against classical diffraction prediction [13] around a rectangular plate in Fig. 16.

It may be observed by comparing fit to measurements to free space that the excess loss due to blockage is about 7 dB at 35 m.

The observed signal power when blocked is still over 10 dB stronger than predicted by diffraction around the obstacle in free space. Scattering from objects in the factory forms a natural alternative path for the signal. The measured peak azimuth angles are shown in Fig. 17 for unobstructed and obstructed (metal plate at 2 m from the transmitter) cases in the factory aisle. The symbols for each arrival are color-coded to indicate its power in dB relative to peak arrival, as per color bar on the right. It is found that in 65% of the locations, the peak azimuth in the obstructed case (marker x) was within the 10° beamwidth of the peak azimuth in the unobstructed case, implying that even if the direct LOS is blocked, no beam adaptation is needed in 65% of the cases measured. In a few locations around the 20 m range in Fig. 17, scattered arrivals (around 45°) exceeded the power of the LOS arrival (around 180°) by a fraction of decibels. Measurement of azimuthal spectra allows estimates of performance of antennas wider than the 10° antenna used in data collection. When the aisle is thus blocked, using a fixed 90° sector antenna aimed "down the aisle" would lead to under 2 dB misalignment loss for 90% of links compared to adaptive 90° beam tracking peak directions.

Similar measurements for blocking object 10 m in front of the Tx are shown in Fig. 18, where we observe much weaker effect of blockage, within 2 dB of free-space loss.

In summary, a 1.7 m × 1 m obstacle as close as 2 m from the terminal produces up to 7 dB reduction in received signal strength and does not require beam adaptation in 65% of the cases. Blockage at larger distances creates even smaller losses.

The average loss caused by blockage for NLOS links was observed to be around 1 dB, much smaller than the spread of the measurement data itself. This is likely because the obstruction does not block a substantial part of the multiple paths for NLOS links.

VIII. Coverage Assessment and Deployment Recommendations

We provide coverage estimates and deployment recommendations for factories at 28 GHz. We consider a private 5G network in a 100 m × 100 m factory with a 28 GHz AP attached to the ceiling at 3 m height in the middle of the factory, at the intersection of two central aisles. The AP has 25 dBm transmit power per polarization, supporting 2 × 2 MIMO via dual polarization. The bandwidth of 400 MHz contains many coherence bandwidths,[1] thus providing frequency diversity against fast fading. Terminals in the central aisles, such as delivery robots, are in LOS to the AP, while terminals in the rest of the factory, such as machines and assembly robots, are in NLOS.

Path gain models and gain degradation models are derived from our extensive measurement campaigns. More specifically, the LOS path gain model is from Fig. 2, while NLOS links are modeled by the joint NLOS path gain model

[1]The median delay spread in a 100 m × 100 m factory is estimated to be 35 ns as per [3], corresponding to coherent bandwidth of about 30 MHz.

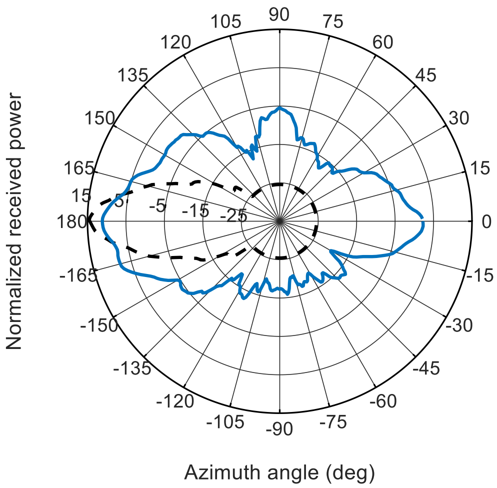

Fig. 10. Sample received azimuthal power profile in LOS factory aisle (solid) and in an anechoic chamber (dashed).

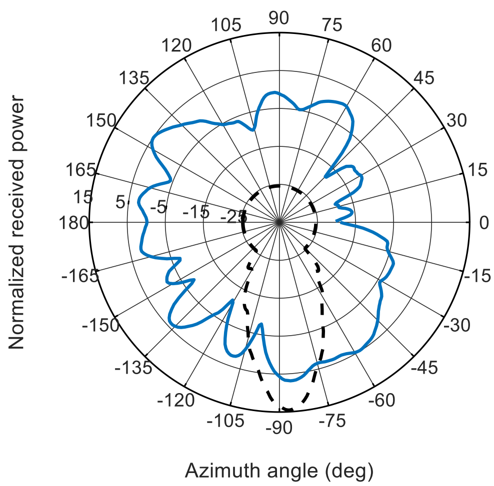

Fig. 11. Observed power azimuth spectrum in NLOS in Factory 1 (solid) and in an anechoic chamber (dashed).

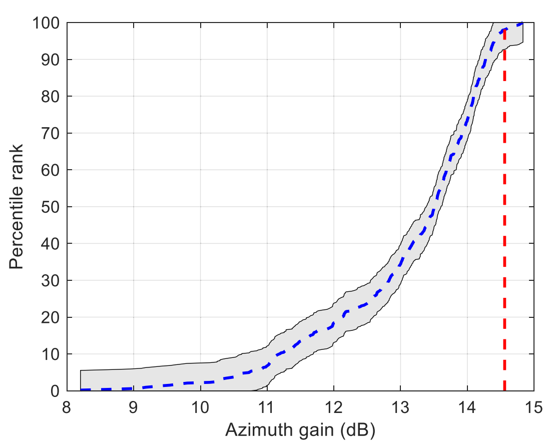

Fig. 12. Distribution of measured azimuth gain across all LOS links. The gray area indicates 90% confidence interval [10] and the vertical red dashed line is the nominal azimuth gain as obtained in an anechoic chamber.

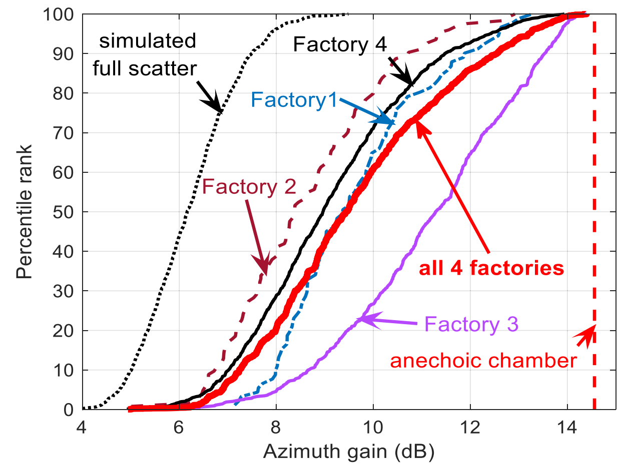

Fig. 13. Observed distributions of effective azimuth gain in NLOS factory links at 2.3–2.6 m height.

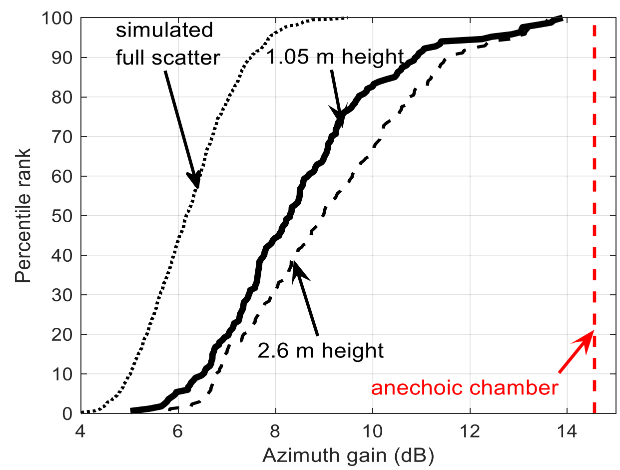

Fig. 14. Azimuth gain distribution measured in Factory 4 at the same set of (x, y) locations, at 1.05 and 2.6 m heights.

from Fig. 7 as broadly representative of diverse factory environments. Azimuth gain degradation is derived from Fig. 13. For coverage prediction, we assume that the angular spread model for elevation is the same as for azimuth. This likely reduces the available effective gain if the elevation spread is less than the azimuth spread, as recommended by 3GPP in other environments [3].

We evaluate downlink (DL) rates with a terminal noise figure of 10 dB. Time-division duplexing with 80% DL ratio is assumed, with cell throughput evaluated as truncated Shannon rates with 3 dB implementation penalty and SNR cutoff threshold of -10 dB, a standard practice for 3GPP system-level simulation to eliminate links with spectral efficiency below the corresponding threshold [12]. It is assumed that a single AP is serving the entire factory, one terminal at a time.

Either omni or directional antennas can be used at the AP and the terminal. One example is to equip the AP with four phased array antenna panels, each covering a 90° sector, either using a fixed wide beam (90° in azimuth, 30° in elevation, 11 dBi) or electronically steered narrow beams (23 dBi, 12°) within the sector. The coverage estimates in terms of CDFs of DL cell throughput are presented in Fig. 19, and the DL coverage range (achieving at least -10 dB SNR) as well as cell edge (10%) throughput are summarized in Table IV.

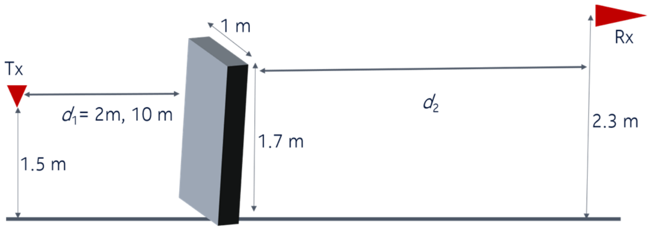

Fig. 15. Blocked geometry in a factory aisle.

TABLE IV
DL Coverage Range and Cell Edge Throughput

AP antenna	Terminal antenna	DL coverage range (-10 dB SNR)	DL edge (10%) throughput
Omni	Omni	28 m	Outage
11 dBi	Omni	45 m	70 Mbps
23 dBi	Omni	64 m	130 Mbps
23 dBi	10 dBi	> 70 m	600 Mbps

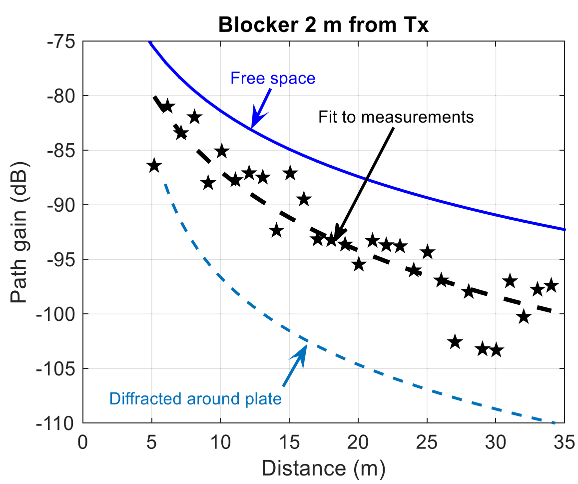

Fig. 16. Path gain measured in a factory aisle with LOS blocked by a 1.7 m × 1 m metal plate, placed 2 m from the Tx.

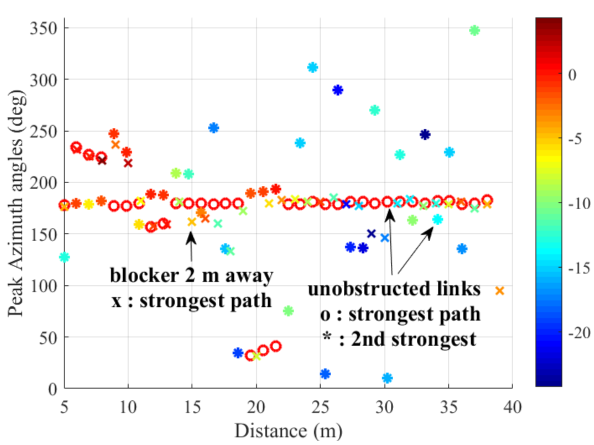

Fig. 17. Measured azimuth directions for strongest obstructed (x), strongest unobstructed (o), and second strongest unobstructed (*) arrivals. "Obstructed" refers to a metal plate 2 m from the transmitter.

The simplest approach, deploying omni antennas at both ends, has over 10% of users in outage. Using a fixed beam antenna (11 dBi) at the AP improves the DL coverage range

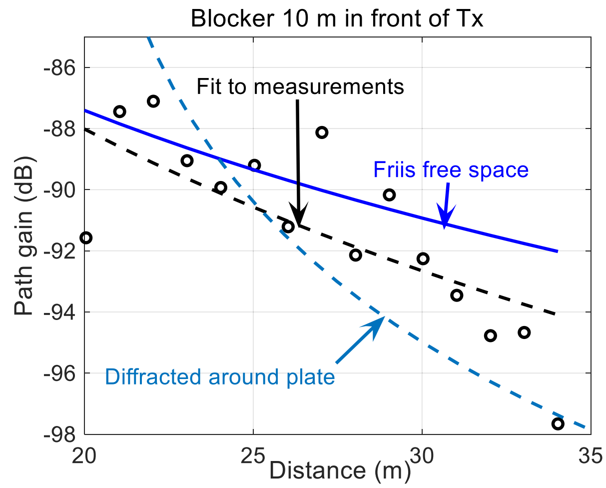

Fig. 18. Measured path gain with 1.7 m × 1 m object blocking the LOS in a factory aisle, 10 m from the Tx.

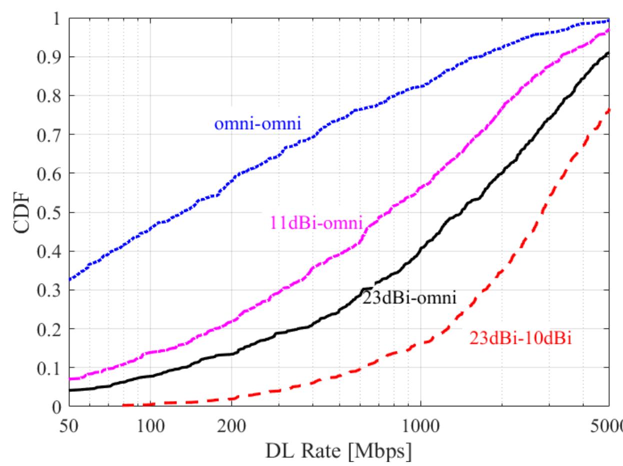

Fig. 19. CDF of DL cell throughput under three different AP-terminal antenna settings.

to 45 m with 70 Mb/s DL cell edge throughput, assuming uniform spatial distribution of terminals. This simple solution does not require beam pointing toward a terminal. Using a 23 dBi (12°) AP antenna capable of pointing beams toward a terminal improves the DL coverage range to 64 m and DL cell edge throughput to 130 Mb/s. Further improvement can be obtained by using a directional antenna at the terminal. For example, with a 10 dBi (55°) terminal antenna, 600 Mb/s DL edge throughput can be delivered.

Impact of blockage is only significant for LOS links at a short distance to terminals: up to 7 dB loss was observed when a 1.7 m × 1 m metal plate placed at 2 m from terminal and the loss for NLOS links is negligible. Since the LOS links have very high SNR, and they only account for about 8% of all links (assuming that the aisles are 3–4 m wide), such extra 7 dB blockage margin for LOS links does not change the cell edge throughput.

IX. Conclusion

Directional measurements of over 2000 links in four-factory environments were collected at 28 GHz and, partially, at 3.5 GHz, to characterize coverage at ranges exceeding 100 m. Key results obtained from these measurements are given as follows.

1) Path gain and azimuth gain models derived from extensive and diverse measurements allow reliable estimates of 90% coverage in factories. The corresponding 3GPP path gain models are found to predict 6–10 dB less loss than the measured one here.
2) Azimuth spreads up to 26° for 90% of links correspond to azimuth gain degradation of 7.3 dB suffered by the 10° horn antenna used.
3) A simple, theoretically derived expression for path gain, dependent on ceiling and clutter heights, is found to represent path gain with an RMSE of 4.4 dB, contrasted with 6.9 dB RMSE from the overall linear fit and 8.7–15.0 dB RMSE from the 3GPP inF models. The new theoretical model maintains its accuracy against available 3.5 GHz factory path gain data, with 3.3 dB RMSE.
4) LOS blockage by a 1.7 m × 1 m obstacle in a factory aisle as close as 2 m from the terminal produces up to 7 dB reduction in received signal strength and does not require beam adaptation in 65% of the cases. Blockage at larger distances creates even smaller losses.
5) Estimation of coverage using antennas with practical gains in realistic conditions provides a way to assess the value of using directional antennas in a scattering environment. It is found that an AP using 25 dBm transmit power per polarization, with 23 dBi nominal gain and omnidirectional terminals, supporting 2 × 2 MIMO in 400 MHz bandwidth, can provide 130 Mb/s for 90% of factory locations within 50 m at 28 GHz.
6) The overall coverage planning can be made specific to a particular factory using its clutter and ceiling heights, making use of the accurate theoretical path gain formula presented here.

Measured factory areas did not have wall separations, which, if present, are expected to alter the propagation characteristics, becoming both obstacles as well as sources of reflection.

Acknowledgment

The authors would like to thank J. Kruse, T. Schlitter, F. Schaich, T. Wild, S. Khosravirad, Lassi Leiden, and Heikki Romppainen for their excellent support during the measurement campaigns and for the helpful discussions.

References

[1] D. Chizhik, J. Du, R. A. Valenzuela, J. Otterbach, R. Fuchs, and J. Koppenborg, "Path loss and directional gain measurements at 28 GHz for factory automation," in *Proc. IEEE Int. Symp. Antennas Propag. USNC-URSI Radio Sci. Meeting*, Atlanta, GA, USA, Jul. 2019, pp. 2143–2144.
[2] D. Chizhik *et al.*, "Diffusion model for cluttered industrial environments at 28 GHz," in *Proc. IEEE Int. Symp. Antennas Propag. North Amer. Radio Sci. Meeting*, Montreal, QC, Canada, Jul. 2020, pp. 1173–1174.
[3] *Study on Channel Model for Frequencies From 0.5 to 100 GHz*, 3GPP, document TR 38.901 V16.1.0, 2019.
[4] R. Candell *et al.*, "Industrial wireless systems: Radio propagation measurements," NIST, Gaithersburg, MD, USA, Tech. Rep., 1951, Jan. 2017.
[5] J. T. Quimby *et al.*, "NIST channel sounder overview and channel measurements in manufacturing facilities," NIST, Gaithersburg, MD, USA, Tech. Rep., 1979, Nov. 2017.
[6] D. Chizhik, J. Du, R. Feick, M. Rodriguez, G. Castro, and R. A. Valenzuela, "Path loss and directional gain measurements at 28 GHz for non-line-of-sight coverage of indoors with corridors," *IEEE Trans. Antennas Propag.*, vol. 68, no. 6, pp. 4820–4830, Jun. 2020.
[7] J. S. Lu, H. L. Bertoni, K. A. Remley, W. F. Young, and J. Ladbury, "Site-specific models of the received power for radio communication in urban street canyons," *IEEE Trans. Antennas Propag.*, vol. 62, no. 4, pp. 2192–2200, Apr. 2014.
[8] D. Chizhik, J. Du, R. Feick, and R. A. Valenzuela, "Theoretical path loss model for suburban fixed wireless access and comparison against 28 GHz measurements," in *Proc. 13th Eur. Conf. Antennas Propag. (EuCAP)*, Krakow, Poland, 2019, pp. 1–3.
[9] D. Chizhik and J. Ling, "Propagation over clutter: Physical stochastic model," *IEEE Trans. Antennas Propag.*, vol. 56, no. 4, pp. 1071–1077, Apr. 2008.
[10] A. Dvoretzky, J. Kiefer, and J. Wolfowitz, "Asymptotic minimax character of the sample distribution function and of the classical multinomial estimator," *Ann. Math. Statist.*, vol. 27, no. 3, pp. 642–669, Sep. 1956.
[11] D. C. Montgomery and G. C. Runger, *Applied Statistics and Probability for Engineers*, 3rd ed. Hoboken, NJ, USA: Wiley, 2003.
[12] *Study on New Radio Access Technology: Radio Frequency (RF) and Co-Existence Aspects*, 3GPP, document TR 38.803, Sep. 2017.
[13] A. Ishimaru, *Electromagnetic Wave Propagation, Radiation, and Scattering*. Upper Saddle River, NJ, USA: Prentice-Hall, 1991.
[14] D. Chizhik, J. Ling, and R. A. Valenzuela, "Radio wave diffusion indoors and throughput scaling with cell density," *IEEE Trans. Wireless Commun.*, vol. 11, no. 9, pp. 3284–3291, Sep. 2012.

Dmitry Chizhik (Fellow, IEEE) received the Ph.D. degree in electrophysics from NYU, Brooklyn, NY, USA, in 1991. His thesis work was on ultrasonics and nondestructive evaluation.

He joined the Naval Undersea Warfare Center, New London, CT, USA, where he did his research in scattering from ocean floor, geoacoustic modeling of porous media, and shallow water acoustic propagation. In 1996, he joined Bell Laboratories, Holmdel, NJ, USA, with a focus on radio propagation modeling and measurements, using deterministic and statistical techniques. He has been involved in the measurement, modeling, and channel estimation of MIMO channels. The results are used both for the determination of channel-imposed bounds on channel capacity and system performance and for the optimal antenna array design. His recent work has included system and link simulations of satellite and femtocell radio communications and millimeter-wave propagation that included all aspects of the physical layer. His research interests include acoustic and electromagnetic wave propagation and scattering, signal processing, communications, radar, sonar, and medical imaging.

Dr. Chizhik was a recipient of the Bell Labs President's Award and a Distinguished Member of Technical Staff.

Jinfeng Du (Member, IEEE) received the B.Eng. degree in electronic information engineering from the University of Science and Technology of China (USTC), Hefei, China, in 2004, and the M.Sc., Tekn. Lic., and Ph.D. degrees from the Royal Institute of Technology (KTH), Stockholm, Sweden, in 2006, 2008, and 2012, respectively.

He was a Post-Doctoral Researcher with the Massachusetts Institute of Technology (MIT), Cambridge, MA, USA, from 2013 to 2015, and then, he joined the Bell Labs at Crawford Hill, Holmdel, NJ, USA. His research interests include wireless communications, especially in communication theory, information theory, wireless networks, millimeter-wave propagation, and channel modeling.

Dr. Du received the Best Paper Award from the International Conference on Wireless Communications and Signal Processing (IC-WCSP) in 2010. His article was elected as one of the Best 50 articles at the IEEE GLOBECOM 2014. He received the prestigious Hans Werthen Grant from the Royal Swedish Academy of Engineering Science (IVA) in 2011, the Chinese Government Award for Outstanding Self-Financed Students Abroad in 2012, the International PostDoc Grant from the Swedish Research Council in 2013, and three grants from the Ericsson Research Foundation.

Reinaldo A. Valenzuela (Fellow, IEEE) received the B.Sc. degree from the University of Chile, Santiago, Chile, in 1975, and the Ph.D. degree from Imperial College London, London, U.K., in 1982.

He is currently the Director of the Communication Theory Department and a Distinguished Member of Technical Staff with Nokia Bell Laboratories, Murray Hill, NJ, USA. He has authored 190 articles and holds 44 patents. He has over 32 600 Google Scholar citations. He is currently engaged in propagation measurements and models, MIMO/space–time systems achieving high capacities using transmit and receive antenna arrays, HetNets, small cells, and next-generation air interface techniques and architectures.

Dr. Valenzuela is a member of the National Academy of Engineering, a Bell Labs Fellow, a WWRF Fellow, and a Fulbright Senior Specialist. He was a recipient of the IEEE Eric E. Sumner Award, the 2014 IEEE CTTC Technical Achievement Award, and the 2015 IEEE VTS Avant Garde Award. He is a "Highly Cited Author" in Thomson ISI.

Dragan Samardzija received the Ph.D. degree in electrical engineering from the Wireless Information Network Laboratory (WINLAB), Rutgers University, New Brunswick, NJ, USA, in 2004.

Since 2000, he has been with Bell Labs, Murray Hill, NJ, USA, focusing on 5G and now 6G radio access and platforms for the Internet of Things (IoT), cyber-physical systems, ultra reliable low latency communications (URLLC), and time-sensitive networking. He has authored over 50 peer-reviewed publications and has numerous patents granted and pending.

Dr. Samardzija received the Bell Labs Fellow Award in 2017.

Stepan Kucera (Senior Member, IEEE) received the Ph.D. degree in informatics from Kyoto University, Kyoto, Japan, in 2008.

He is currently with Nokia Bell Labs Munich, Munich, Germany, where he works as a 3GPP RAN2 Delegate for sidelink and positioning technologies. Between 2011 and 2020, he was with Nokia as a Principal Researcher and the Project Manager as well as actively participated in large-scale EU research projects totaling 15+ Mil. EUR. His innovations were productized by Nokia and commercially deployed by top-tier customers worldwide as well as demonstrated in industry shows. He has filed nearly 100 patents and has published more than 70 book chapters, transactions, and conference papers in peer-reviewed ACM/IEEE venues.

Dr. Kucera was a recipient of multiple professional awards, among others the Nokia Top Inventor 2018, the Nokia U.K.&I Top Inventor of All Times, the Hummies Gold Award for Best Human-Competitive Design 2019, and the Irish Laboratory Scientist of the Year Award 2018.

Dmitry Kozlov received the B.Sc. and M.Sc. degrees in radiophysics from Saint Petersburg Electrotechnical University LETI, St. Petersburg, Russia, in 2009 and 2011, respectively, and the Ph.D. degree in electronics and electrical engineering from Queen's University Belfast (QUB), Belfast, U.K., in 2016.

He was a Marie Curie Early-Stage Researcher with the Institute of Electronics, Communications and Information Technology, QUB, from 2013 to 2016. He is currently with Nokia Mobile Networks, Ulm, Germany. His research interests include microwave and antenna theory, including synthesis of antenna arrays, and analysis of nonlinear distortions in microwave passive and active devices.

Rolf Fuchs received the M.S. and Dipl.-Ing. degrees in electrical engineering and information technology with a specialization in (tele)communication engineering from the University of Kaiserslautern, Kaiserslautern, Germany, in 2000.

He has been a Research Engineer at Nokia Bell Labs, Stuttgart, Germany, since 2001. He has coauthored research articles and holds issued or pending patents in his area of expertise. His research interests include signal processing, smart antenna, and channel sounding and localization techniques for 5G and 6G.

Juergen Otterbach received the Dipl.-Ing. degree in electrical and information engineering from Technical University Stuttgart, Stuttgart, Germany, in 1987.

In 1988, he started at the SEL Research Center, Stuttgart, on coherent optical transmission, later CATV distribution system using optical fiber amplifiers. He was technically responsible for VoD Field trial in Berlin in 1995 with 50 active subscribers. Since 2001, he has been researching the topics with Sync-CDMA (LMDS) in the 28 GHz band inside the EU project. Since 2005, he has been working for OFDM-based PHY research WiMAX and commercial development, including IEEE802.16m standardization body. Since 2010, he has been working on 4G LTE Advanced prototyping and nowadays focusing on 5G Next Generation Wireless Systems for URLLC and Precise Positioning. He is currently a Research Engineer at Nokia Bell Labs, Stuttgart. He has authored IEEE articles and coauthored multiple articles in journals and international conferences. He holds multiple patents.

Johannes Koppenborg received the Diploma degree in physics from the university in Bochum, Germany, in 1985.

After graduation, he joined Alcatel Research, Stuttgart, Germany. Until 2002, he worked on the development of single-mode fibers and dense wavelength division multiplexing (DWDM) components. In 2003, he started to research on wireless systems for UMTS, HSPA, LTE, and later 5G. Within Nokia Bell Labs, he became responsible for the wireless systems laboratory and field trial team, with a special focus on 5G solution for the industry. In 2019, he became responsible for manufacturing and automotive solution at Nokia CX Digital Industries with a special emphasis on private wireless. He has authored or coauthored more than 25 articles in journals and international conferences.

Paolo Baracca (Member, IEEE) received the B.Sc. and M.Sc. degrees in telecommunications engineering and the Ph.D. degree in information engineering from the University of Padua, Padua, Italy, in 2007, 2009, and 2013, respectively.

He has been a Research Engineer at Nokia Bell Labs, Stuttgart, Germany, since 2013. He has coauthored more than 50 research articles, holds more than 30 issued or pending patents, and regularly serves as a reviewer for IEEE journals and conferences. His research interests include signal processing, multiantenna, and resource allocation techniques for 5G and 6G.

Mark Doll received the Dipl.-Phys. degree in physics from the Technical University of Brunswick, Brunswick, Germany, in 2000, and the Dr.-Ing. degree in computer science from the Karlsruhe Institute of Technology, Karlsruhe, Germany, in 2007.

He is currently a Research Engineer at Nokia Bell Labs, Stuttgart, Germany, focusing on architecture, control algorithms, and signaling aspects, and their implementation for mobile radio access, covering topics from coordinated multipoint transmission reception, split processing, and network slicing, over air-to-ground communication for aircraft and mmWave communication for high-speed trains, to most recently joint communication and sensing.

Ignacio Rodriguez (Member, IEEE) received the B.Sc. and M.Sc. degrees in telecommunication engineering from the University of Oviedo, Oviedo, Spain, in 2016, and the M.Sc. degree in mobile communications and the Ph.D. degree in wireless communications from Aalborg University, Aalborg, Denmark, in 2011 and 2016, respectively.

He is currently an Assistant Professor with Aalborg University, where he leads the 5G for Industries Research Group. He is also an External Research Engineer with Nokia Bell Labs, where he is mainly involved in 3GPP and ITU-R standardization activities. His research interests include radio propagation, channel modeling, ultrareliable and low-latency communications, and the industrial Internet of Things (IoT).

Dr. Rodriguez was a co-recipient of the IEEE VTS 2017 Neal Shepherd Memorial Best Propagation Paper Award, and in 2019, he was co-awarded with the 5G-prize by the Danish Energy Agency and the Danish Society of Telecommunication Engineers.

Rodolfo Feick (Life Senior Member, IEEE) received the Ingeniero Civil Electronico degree from Universidad Técnica Federico Santa María (UTFSM), Valparaíso, Chile, in 1970, and the Ph.D. degree in electrical engineering from the University of Pittsburgh, Pittsburgh, PA, USA, in 1975.

Since 1975, he has been with the Department of Electronics Engineering, UTFSM, where he is currently an Associate Researcher. His current research interests include RF channel modeling, digital communications, microwave system design, and RF measurement.

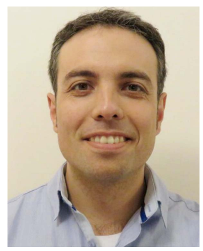

Mauricio Rodriguez (Senior Member, IEEE) received the Ingeniero Civil Electronico, M.Sc., and Ph.D. degrees in electronics engineering from Universidad Técnica Federico Santa María, Valparaíso, Chile, in 2011, 2011, and 2017, respectively.

He has been with the Escuela de Ingeniería Eléctrica, Pontificia Universidad Católica de Valparaíso, Valparaíso, since August 2016. His main research interests include RF channel modeling, RF measurement, and microwave system design.